TD-09-015

First Tests of a Prototype Optical System for the HINS Focusing Solenoid Alignment Study

Warren Schappert
Test and Instrumentation Department
Technical Division
Fermilab

August 30, 2009

Abstract

This note describes results from the first test of a prototype optical auxiliary alignment system for the HINS superconducting solenoids. The alignment system is designed to track transverse displacements of the solenoids as the cryomodule is cooled 4K. During operation, the transverse displacement of the magnetic axis of each solenoid must be kept within ±300μm of the beam axis. Tests indicate that the prototype system can track transverse displacements of the solenoid to 10 μm. Rotations of the solenoid can be tracked to 100 μrad or better.

Introduction

Beam line components must be aligned to tight tolerances during assembly and installation and that alignment must be maintained during operation. Accurate alignment of superconducting components within a pressure vessel is difficult using conventional survey and alignment equipment.

To circumvent these difficulties, auxiliary alignment systems using a stretched wire have been used to establish the displacement of superconducting beam-line components from a reference line and to transfer those displacements to an external coordinate system. Component locations relative to the wire are determined by RF or optical sensors inside the cryomodule.

The most widely used auxiliary alignment system is the wire position monitor (WPM). An RF WPM system built by INFN has been successfully used to track displacements of internal components during thermal cycles of Tesla cryomodules at DESY. The INFN system can achieve a resolution of 10 μm [1] but systematic uncertainties due to gravitational wire sag, wire vibration and uncertainties in the readout calibration, limit the overall precision of the system to 100 μm [2].

Laser based systems offer significantly better accuracy at a lower cost and reduced complexity. Beginning in 1988, SLAC developed an alignment system using a HeNe laser and large Fresnel zone plates. This system was used to align the linac components to an accuracy of 25μm over a distance of 3km [3]. Although the SLAC system provided impressive accuracy, the Fresnel plates were mechanically switched in and out of the laser beam making such a system unsuitable for use inside a cryomodule.

The ideal auxiliary alignment system would:

1) Provide micron accuracy and position linearity;
2) Provide micron stability over the lifetime of the cryomodule;
3) Require no moving mechanical parts inside the vacuum;
4) Require no active electronic components inside the vacuum; and
5) Require little or no cabling inside the cryomodule.

Low cost laser diode modules and CCD and CMOS cameras are currently available for a small fraction of the cost of the RF electronics required to sense the position of a stretched wire (the cost of a complete stretched wire system estimated to be $100K per cryomodule). Commercially available cameras offer pixel sizes ranging from several microns to several tens of microns and digital processing techniques make it possible to determine the centroid of a laser beam with sub-pixel precision. These devices cannot operate inside a cryomodule, but as internal components move, retroreflectors can be used to displace a laser beam or beams in such way that the component displacements can be tracked by external cameras.

This note describes the first bench tests of a prototype optical system that uses retroreflectors and CMOS cameras to track the position of components inside the HINS cryomodule. No active components or cabling are required inside the vacuum.

Proposed Optical Scheme

The optical scheme of the prototype system is shown schematically in Figure 1. A narrow laser beam is projected into the system through a beam splitter. A portion of the primary beam is reflected back into the first of two CCD cameras. The camera records position of the laser beam at the entrance to the system. The remainder of the primary beam is directed through a partial retroreflector attached to a component inside the cryomodule. The retroreflector reflects a portion of the primary beam back along the direction of arrival but offset in space. The spatial offset is proportional to the distance of the incident

beam from the axis of symmetry of the retroreflector. The position of the retro-reflected beam is also captured by the first camera.

The portion of the primary beam passes un-reflected through the partial-retroreflector is captured by a second camera at the other end of the cryomodule.

The locations of the primary beam spots in the two cameras at either end of the cryomodule define a reference line that can be easily connected to the beam-line reference coordinate system.

As the components inside the cryomodule shift during a thermal cycle, the spatial offset between the retro-reflected beam and the primary beam will change. By tracking the location position of the retro-reflected beam spot in the first camera, the motion of the component can be recovered.

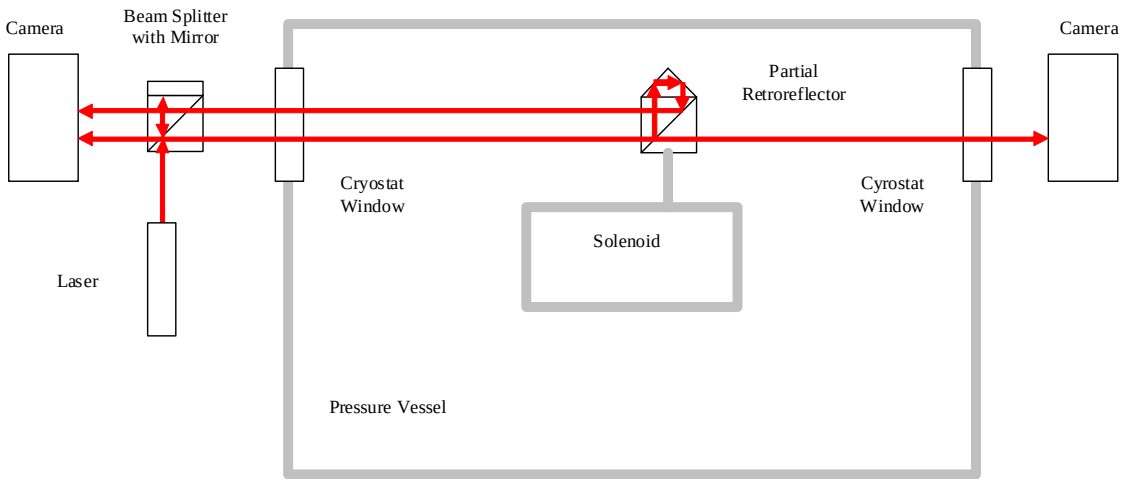

Figure 1: Optical Scheme for a Proposed Alignment System for the HINS Solenoids.

System Sensitivity Analysis

The overall accuracy and resolution of the system will be determined by:

- The accuracy with which the position of the cameras can be determined;
- The accuracy with which the beam spot position can be determined from the camera images; and
- Any deflections or spatial offsets of the laser beam by the optical components of the system.

Translation stages are commercially available with bidirectional repeatability specifications of 2 µm [4], and commercial CCD laser position monitors are available with accuracies of 5 um deviation edge to edge over the aperture of the sensor [5].

Although, unlike a stretched wire, the laser beam will not sag due to gravitation, it may be deflected or offset each time it passes through an optical component or window. As shown schematically in Figure 2, a component with an optical axis that is not perpendicular to the incident beam will spatially offset the beam. A component with exit and entry faces that are not parallel will deflect the beam.

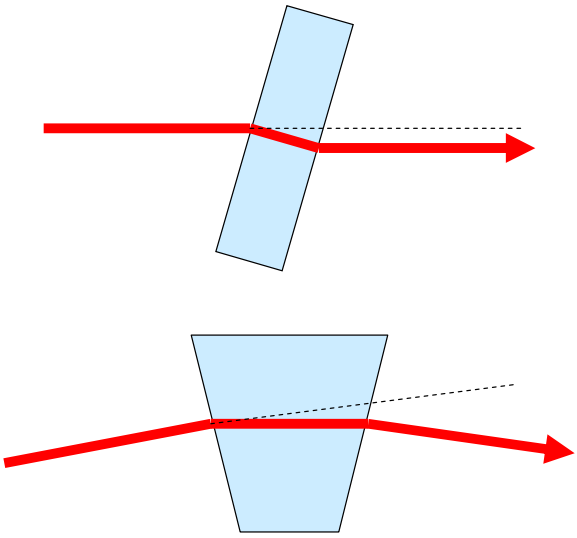

Figure 2: Optical Angular and Parallelism Errors

The combined sensitivity of the system to tolerances of the optical components for cryomodules of lengths 1.5m and 9m is outlined in Table 1 and Table 2 respectively. Optical components were assumed to be aligned with the beam axis to 1 mrad or better. With the exception of the optical windows, a parallelism tolerance of 1 arcsecond (4.8 µrad), was assumed for all components. For the windows a parallelism tolerance of 3 arc seconds [6] was assumed. The beam displacements and deflections due to the tolerances of individual components were added in quadrature to obtain estimates of the resulting uncertainty in the system position determination.

Table 1: Optical Tolerances for a 1.5 m Cryomodule

Component	Displacement Error (um)	Parallelism (mrad)	Z (m)	Parallelism Error (um)	Tilt (mrad)	Thickness (mm)	Displacement Due To Tilt (um)	Combined Error (um)
Camera	5		0	0			0	**5**
Stage	2		0	0			0	**2**

Optical Window		0.015	0.05	1	1	25	8	**8**
Corner Cube		0.005	0.75	4	1	12	4	**6**
Optical Window		0.015	1.45	1	1	25	8	**8**
Stage	2		1.5	0			0	**2**
Camera	5		1.5	0			0	**5**
Total	**8**			**4**			**12**	**15**

Table 2: Optical Tolerances for a 9m Cryomodule

Component	Displacement Error (um)	Parallelism (mrad)	Z (m)	Parallelism Error (um)	Tilt (mrad)	Thickness (mm)	Displacement Due To Tilt (um)	Combined Error (um)
Camera	5		0	0			0	**5**
Stage	2		0	0			0	**2**
Optical Window		0.015	0.05	1	1	25	8	**8**
Corner Cube		0.005	4.5	23	1	12	4	**23**
Optical Window		0.015	8.95	1	1	25	8	**8**
Stage	2		9	0			0	**2**
Camera	5		9	0			0	**5**
Total	**8**			**23**			**12**	**27**

The analysis shows that for a 1.5 m cryomodule the position uncertainty due to optical tolerances is dominated by the tilt of the optical windows. For a 9 m cryomodule, the parallelism of the retroreflector in the center of the cryomodule dominates. In either case, the uncertainty due to tolerances in the optical components is less than 30 µm.

Bench Test Setup

An initial bench test to validate the concept has been conducted. The output of a 635 nm Newport Model LOA-1 alignment laser was focused into a single mode optical fiber using a Thorlabs FC280FC-B collimator. The output of the fiber was re-collimated into a 3mm diameter Gaussian primary beam using a second Thorlabs FC280FC-B. The primary beam was split into two back to back beams using an Edmund Model 5411 12.5mm beam splitter in combination with a plane mirror.

One of the two back-to-back beams exiting the splitter was projected directly into a AVT Stingray F-046B Monochrome CCD camera through a reversed Edmunds Model NT55-577 5x beam expander. The reversed beam expander increased the effective aperture of the camera while improving the match between the pixel size and the target resolution of the system.

The second beam exiting the splitter was projected through a partial retroreflector. The retro-reflected beam was projected back into the first camera while the transmitted beam was projected into a second AVT Stingray F-046B camera through another reversed NT55-577 5x beam expander. Both cameras were equipped with Thorlabs FL635-10 laser line filters to reduce stray light and with neutral density filters to prevent the laser beam from saturating the CCD sensors. The two cameras were separated by 1m and the partial retroreflector was mounted on a micrometer stage positioned half-way between the two cameras.

Two tests were conducted using different retroreflectors. The first test used an Edmund Optics model 43296 12.5 mm corner cube retroreflector. Further tests used a cat's eye retro-reflector consisting of an Edmunds NT49-660 aspheric lens in combination with a Thorlabs Model CM127-012-P01 concave lens.

The partial retroreflector was scanned horizontally through the primary beam in 200 steps of 25.4 µm each using a micrometer stage. At each step of the scan, an image from the each of the two cameras was captured using Matlab to call an Mex routine that wrapped the Intek FileGrab API libraries that were bundled with the AVT cameras.

Beam Spot Tracking

The top row of Figure 3 shows the raw image from ten frames captured by the first camera as the retroreflector was scanned through the primary laser beam using the micrometer stage. In these images two beam spots are visible. The more prominent spot due to the primary beam remains stationary as the retroreflector is scanned. The less prominent spot moves vertically through the primary spot as position of the retroreflector changes with respect to the primary beam.

The second row of Figure 3 shows the images after the primary beam spot has been subtracted. The contribution of the primary beam to each pixel was estimated by taking the median value over the 200 images collected. The median background estimate was then subtracted from each of the images. The subtraction procedure suppresses most of the primary beam leaving a well defined secondary beam.

Although the beam entering the system is Gaussian, both the primary or secondary beams reflected into the camera have been distorted by the corner reflector and are broken into several distinct partial beams. The relative intensities of the partial beams change

throughout the scan. This makes it difficult to determine the position of the secondary beam spot using a simple centroid calculation.

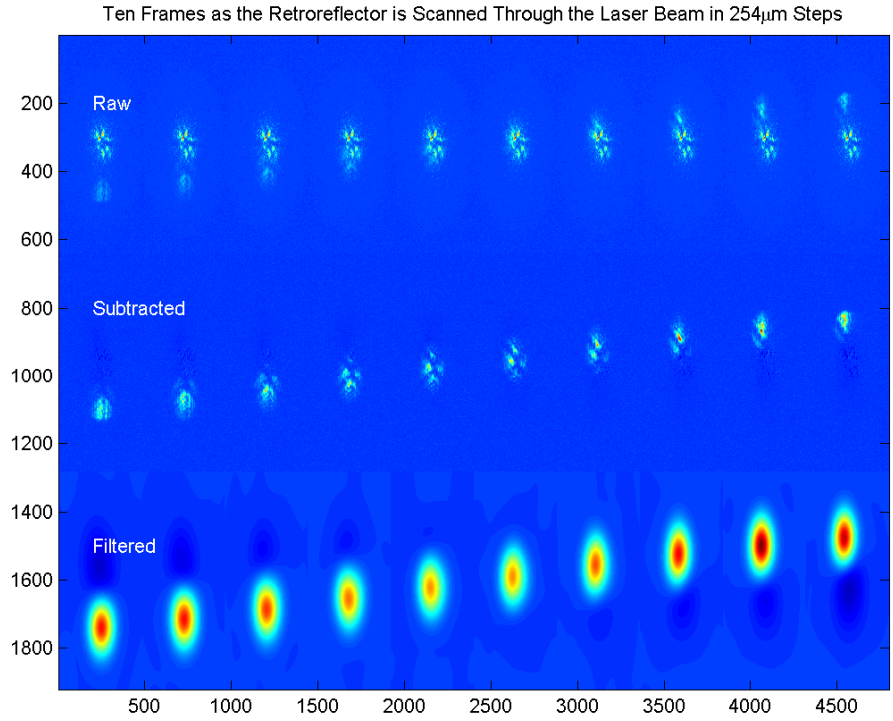

Figure 3: Ten Frames Captured as the Retroreflector is Scanned Through the Laser Beam.

To improve the centroid determination, the subtracted images were convolved with a digital Gaussian filter to combine the partial beams into a single secondary peak, and a trimmed centroid was calculated using only pixels that contained more than 50% of the energy of the peak pixel in the filtered image. The last row of Figure 2 shows the filtered images for the same ten selected frames.

To reduce distortions of the beam spot, the corner cube retroreflector was replaced with a cat's eye retroreflector consisting of a 0.5" aspheric lens with a concave mirror at the focal point of the lens. As shown in Figure 4, light entering the lens is focused onto the mirror and reflected back along the same direction, but offset in space. The offset is proportional to the distance of the incident beam from the axis of symmetry. To achieve the maximum field of view, the radius of curvature of the mirror should be equal to the focal length of the lens [7].

Figure 5 shows an unprocessed image of the primary and retro-reflected beam spots using a cat's eye. In contrast to the spots obtained using the corner cubes, the beam spots consist of a single well defined lobe.

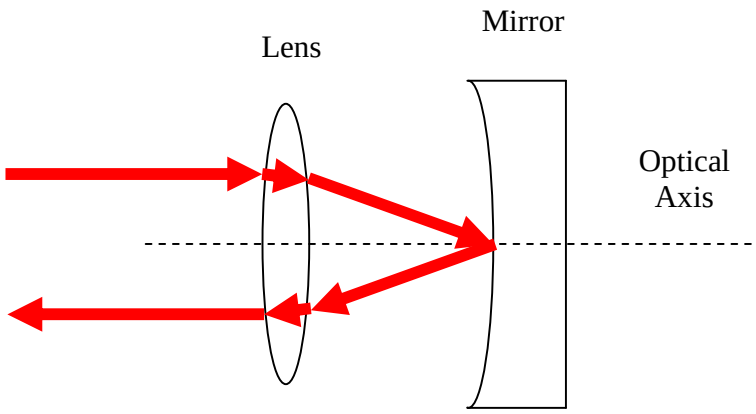

Figure 4: Cat's Eye Retroreflector

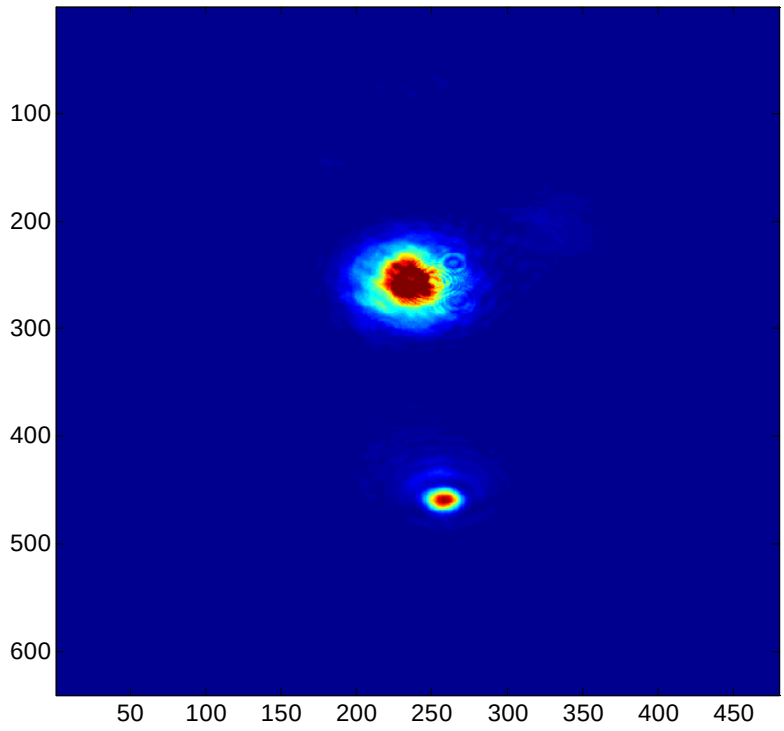

Figure 5: An Unprocessed Image Frame Using the Cat's Eye Retroreflector

As with the corner cube retroreflector, the cat's eye was scanned horizontally through the laser beam using a micrometer stage and the motion of the secondary beam spot was reconstructed as described above. The scan was repeated several times for different vertical displacements.

The acquisition of the scans was semi-automated. The computer would emit a beep each 3 seconds and the operator would step the micrometer by one graduation (25.4 μm). In several instances, scan steps were either missed entirely or the target graduation was overshot. These errors were cumulative over each scan. Furthermore, the 6-axis mount which was used to displace the retroreflector vertically was not as precise as the horizontal micrometer stage and also tilted the retroreflector slightly when the vertical displacement was changes. The impact of these acquisition limitations on the final results is discussed in more detail in the appropriate sections.

Coordinate System Alignment

Figure 6 shows the reconstructed positions of the primary and retro-reflected beam spots. All of the measurements of the primary spot are clustered in a small region, 20 μm in diameter.

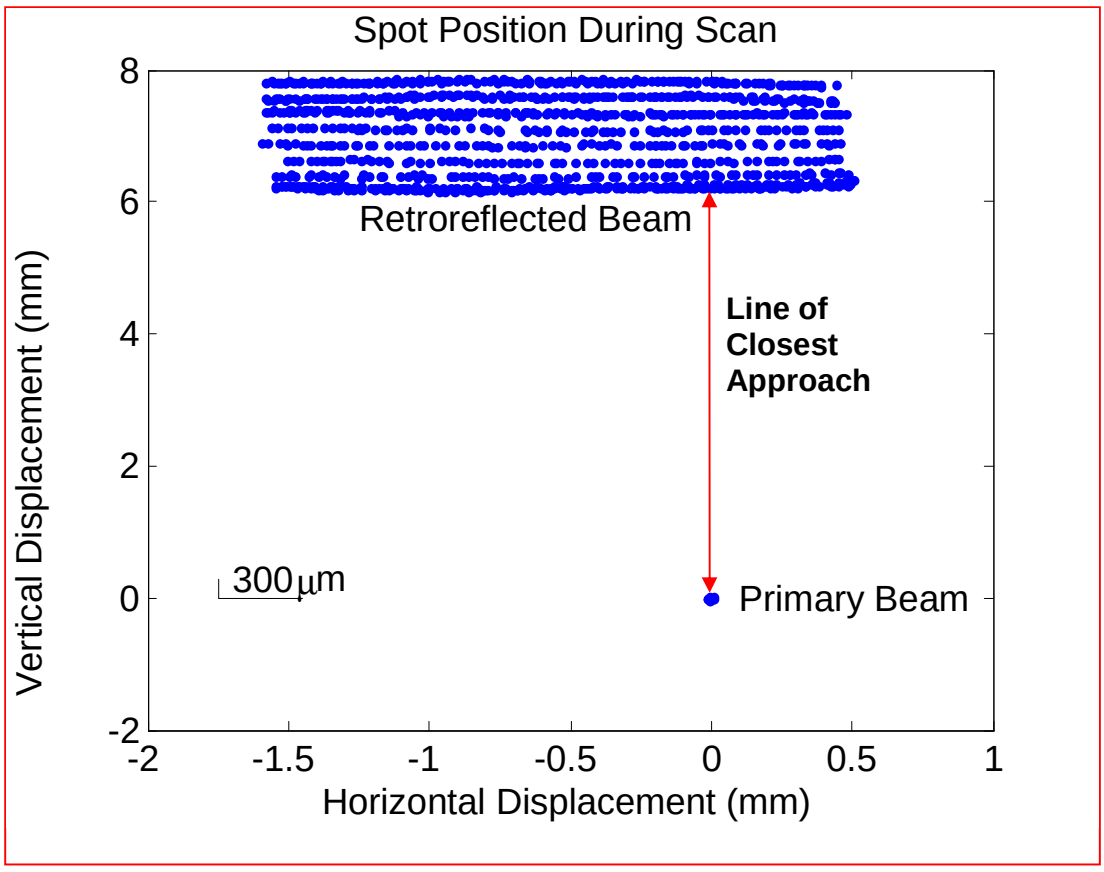

Figure 6: Reconstructed Spot Position of the Primary and Retro-reflected Beams as the Cat's Eye Partial Retroreflector is Scanned through the Primary Laser Beam

No attempt was made to mechanically align the cameras with the coordinate system of the micrometer stage. Instead the spot position data was shifted so that by definition, the average position of the primary beam spots was the origin. The spot data was then rotated

about the origin such that the direction of motion of the spot averaged over all scans was perpendicular to line of closest approach between the scans and the averaged primary beam spot position.

The coordinate system was scaled so that the median displacement between successive scan points was 25.4 μm, the scan micrometer step-size. Points at the extreme left edge of the scan were ignored because of obvious clipping of the beam by the aperture of the retro-reflector.

In the resulting coordinate system, the horizontal position of the retro-reflected beam will be equal and opposite to the distance horizontal distance between the primary beam and the optical axis of the retroreflector. The vertical position of the retro-reflected beam will be equal to twice the vertical distance between the primary beam and the optical axis of the retroreflector.

Linearity

The reconstructed positions of the retro-reflected beam spots are shown in finer detail in Figure 7. Obvious barrel distortion is apparent. To estimate the distortion, the coordinates of the spots in each scan were fit to a quadratic function of the micrometer displacement. These fits are shown by the thin solid lines on the Figure. In the cases that scans were repeated at the same vertical offset, two solid lines are shown. For comparison with the HINS requirements, 300 μm vertical and horizontal bars are also shown.

The barrel distortion it is less than 84 μm maximum over the 2x2 mm scanned aperture. This distortion is likely due to physical clipping of the 3 mm laser beam by the 12.5 mm diameter aperture of the retroreflector, and could likely be reduced by using a 1” diameter cat’s eye.

While multiple scans at the same vertical displacement track each other to much better than 300 μm, systematic vertical deviations larger than the resolution are apparent. Some of these deviations result from the limited vertical reproducibility of the 6-axis mount used to control the vertical displacement of the retro-reflector. In some instances, the angle of the retroreflector may have been slightly disturbed. Because of these hardware limitations, no attempt has been made to quantify systematic discrepancies in the vertical coordinate.

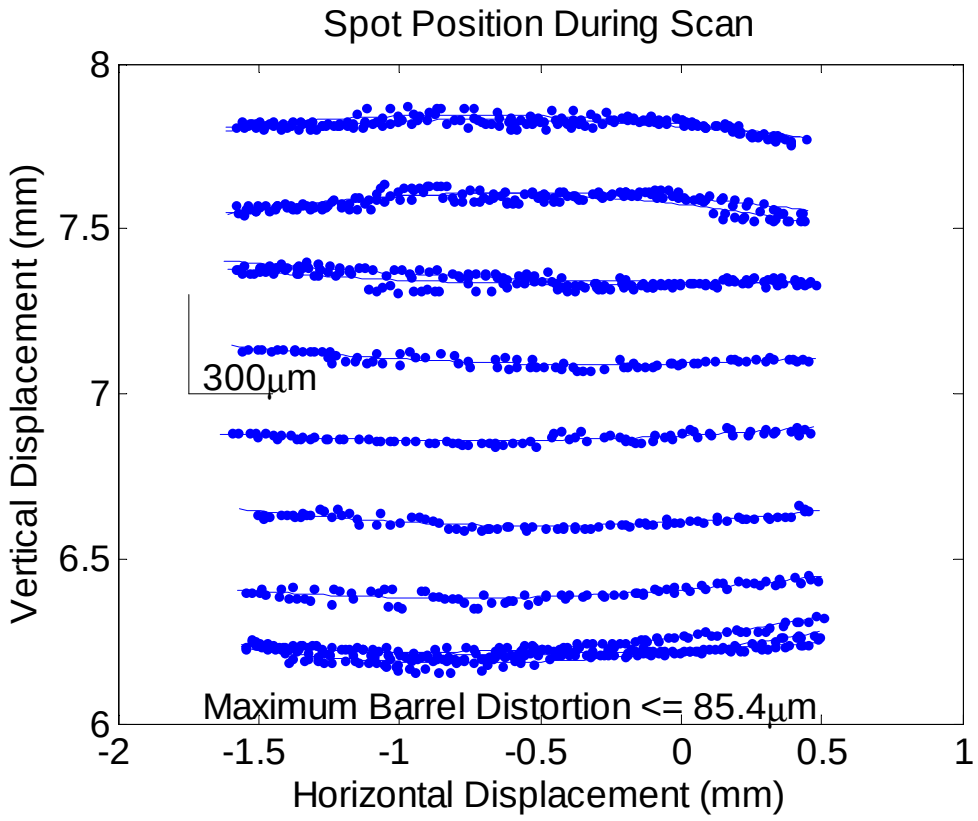

Figure 7:Reconstructed Spot Position of the Retro-reflected Beam as the Cat's Eye Partial Retroreflector is Scanned through the Primary Laser Beam

Resolution

The position resolution of the system was determined by comparing the centroid of the retro-reflected beam spots to the position predicted by the fit for each scan. As shown in Figure 8, the standard deviation is 20.7μm in the horizontal direction and 12.5 μm in the vertical direction.

Because of the limitations in the scanning semi-automated procedure, the horizontal resolution estimate is likely to be overestimates and the vertical discrepancies between scans at the same nominal vertical displacement may be due in all or part to measurement artifacts.

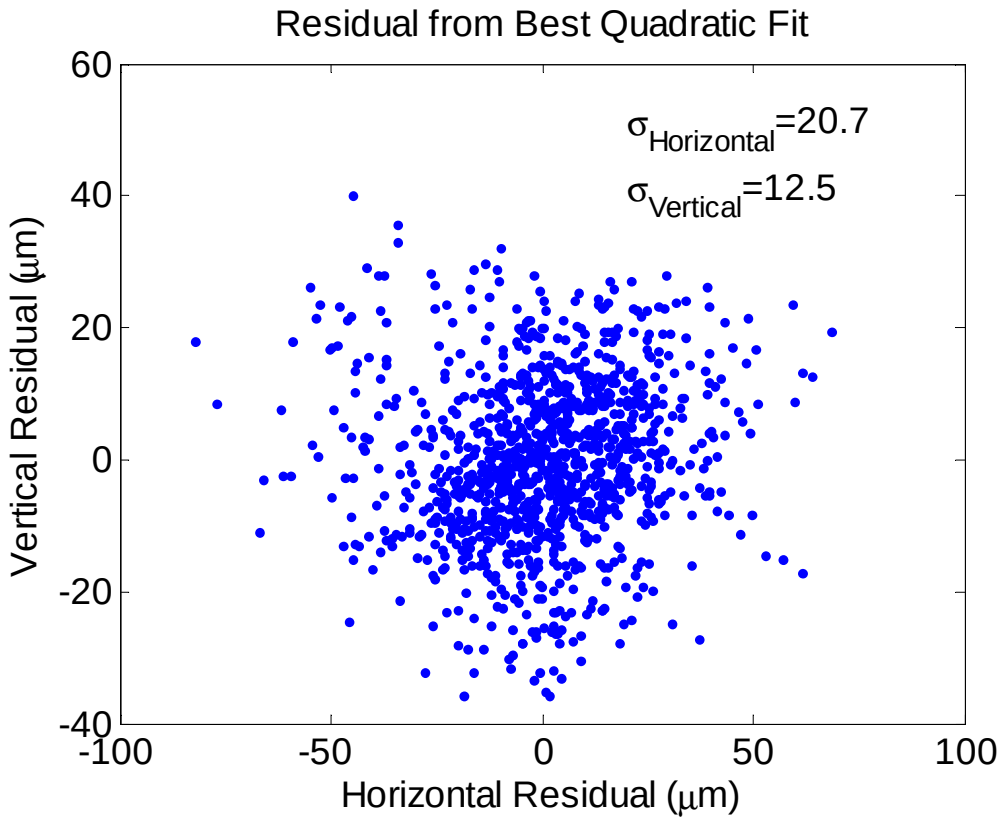

Figure 8:Residuals from the Best Quadratic Fit

Accuracy

Figure 9 shows an expanded view of the data of Figure 6 near the horizontal origin of the coordinate system. The points show the position of the retro-reflected beam spot as measured by the CCD camera for the same horizontal displacement of the retroreflector as measured by the micrometer foreach of the thirteen scans. The horizontal standard deviation of the spot positions, 19.6μm, is a measure of the accuracy with which the symmetry axis of the retroreflector can be determined.

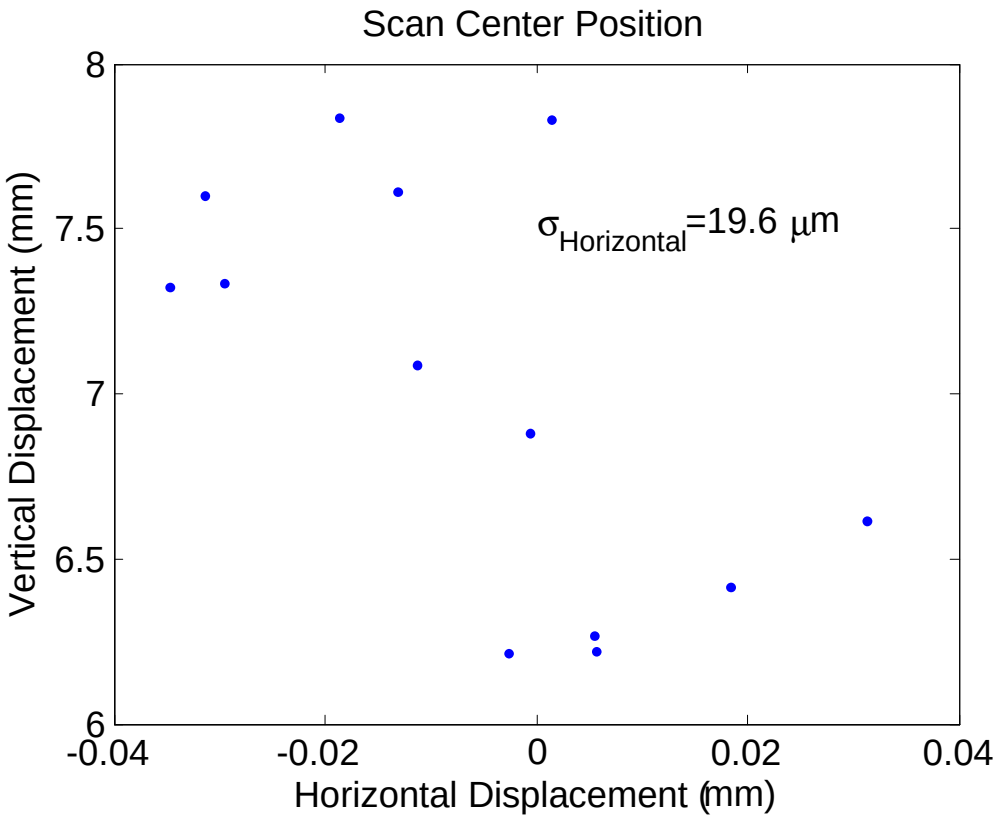

Figure 9: Beam Spot Position for Each Scan When the Micrometer Setting is the Same

Expected System Performance

Figure 11 shows how the system could be used to monitor the position of the solenoid during the cool-down of the cryomodule. Each solenoid has four titanium alignment projecting from the solenoid to a clear optical path through the cryomodule. Cameras attached to external support frames can monitor the position of retroreflectors attached to the end of each of these arms.

The cameras would be mounted on translation stages and the retroreflectors on the front and back arms would be offset vertically so that the location of each retroreflector could be determined independently. For each measurement, the camera positions would be scanned in order to find the optical axis of each retroreflector as shown schematically in Figure 10.

The steps of the procedure are as follows:

1. The first camera is scanned in the horizontal direction and the line of closest approach between the primary beam spot and the path of the retro-reflected beam.
2. The camera is positioned horizontally such that the primary beam spot and the retro-reflected beam spot both lie on the line of closest approach.

3. The camera is moved vertically until the primary and retro-reflected beam spots are a predefined number of pixels apart.
4. The second camera is moved until the centroid position of the primary beam spot is at the center pixel of the sensor.

This procedure ensures that the laser beam always follows the same optical path through the retroreflector and minimizes the uncertainties due to optical effects such a barrel distortion.

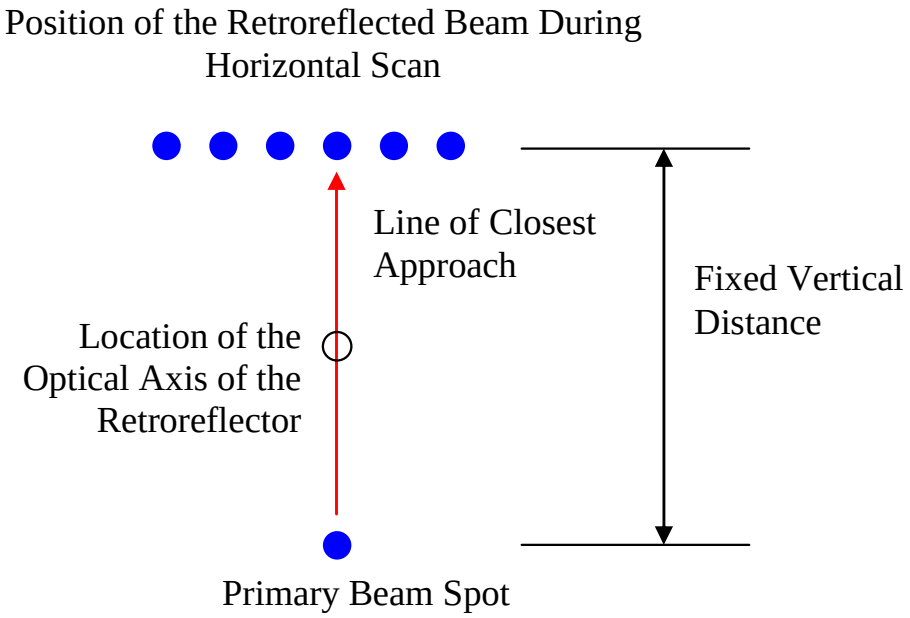

Figure 10: Procedure to Locate the Optical Axis of the Retroreflector

The uncertainties due to parallelism errors of optical components inside the cryomodule may be reduced significantly if the optical aperture is large enough to allow the deflection of the beam to be measured directly. This can be done by scanning the beam and comparing the deflection of the beam as it travels through the component to the deflection of the beam as it travels along a path clear of any components.

The temperature of the support frames should be monitored since thermal expansion can lead to displacements between the cameras of more than the accuracy of the system.

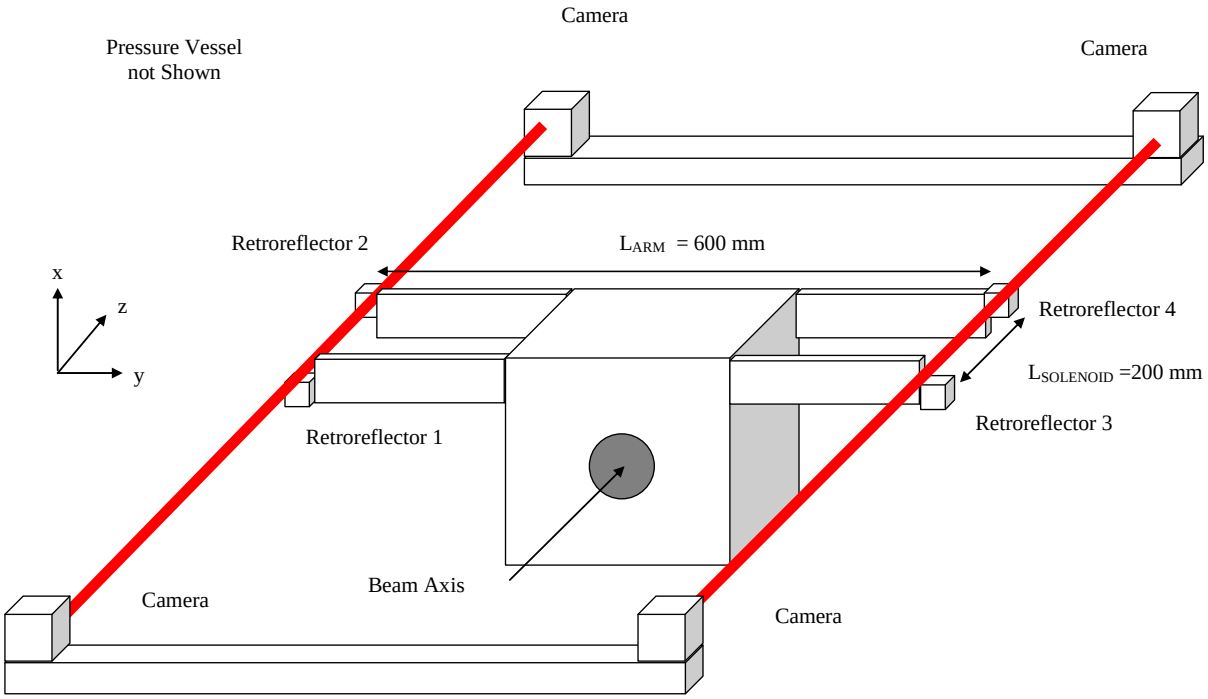

Figure 11: Monitoring the Position of the Solenoid.

Table 3 lists the achievable displacement and angular resolution. The absolute accuracy of the system, i.e. the precision with which the solenoid location can be determined with respect to an external coordinate system, is dominated by the 15 μm uncertainty due to the assumed 1 mrad tilt of the cryomodule optical windows. The differential accuracy, the precision with which the system can track changes in the position of the solenoid during cool down is 10 μm.

Table 3: Solenoid Position and Angular Accuracy Estimates for a Spatial Resolution of 20 μm.

Quantity	Determination	Uncertainty	Value
X Displacement	$(x_1 + x_2 + x_3 + x_4)/4$	$\delta_x / \sqrt{4}$	10 μm
Y Displacement	$(y_1 + y_2 + y_3 + y_4)/4$	$\delta_y / \sqrt{4}$	10 μm
Z Displacement	--	--	--
X-Y Rotation	$(y_1 + y_2 - y_3 - y_4)/(2L_{ARM})$	$20\sqrt{2}/(6x10^5\sqrt{2})$	33 μrad
Y-Z Rotation	$(x_2 - x_1 + x_4 - x_3)/(2L_{SOLENOID})$	$20\sqrt{2}/(2x10^5\sqrt{2})$	100 μrad
Z-X Rotation	$(y_2 - y_1 + y_4 - y_3)/(2L_{SOLENOID})$	$20\sqrt{2}/(2x10^5\sqrt{2})$	100 μrad

Summary

Initial tests of a prototype optical alignment systems show that the optical axis of a cat's eye retroreflector attached can be determined to an accuracy of 20 μm. If a retroreflector is attached to each of the four titanium alignment arms of the HINS solenoid, displacements transverse to the beam can be tracked to 10 μm. Angular displacements can be tracked to 100μrad or better.

References

1. D. Giove et al, A Wire Position Monitor (WPM) System to Control the Cold Mass Movements Inside the TTF Cryomodule, Proc. EPAC 2006, Edinburgh, UK.
2. Analysis Of the Cold Mass Displacements at the TTF. Bosotti,A. et al.; Proc. EPAC 2004, Lucerne, Switzerland
3. http://www.slac.stanford.edu/econf/C06092511/papers/TU013.PDF
4. Thorlabs Corp. MTS50XY-E - MTS50XY Translation Stage http://www.thorlabs.com/NewGroupPage9.cfm?ObjectGroup_ID=3002
5. Melles-Griot Corp., Spot On CCD Optical Beam Position Measurement System, http://www.mellesgriot.com/pdf/SpotOn%20CCD%20Spec%20Sheet.pdf
6. MPF Products Inc., Laser Optics: AR Coated UHV Viewports,http://www.mpfpi.com/catalog/Viewports%206.4.pdf
7. J. J. Snyder , Paraxial ray analysis of a cat's-eye retroreflector. Applied Optics, Vol. 14, Issue 8, (1975) pp. 1825-1828